RETHINKING UNCERTAINTY IN DEEP LEARNING: WHETHER AND HOW IT IMPROVES ROBUSTNESS

Anonymous authors
Paper under double-blind review

ABSTRACT

Deep neural networks (DNNs) are widely known to be prone to adversarial attacks, for which many remedies are proposed. While adversarial training (AT) is regarded as the most robust defense, it suffers from poor performance both on clean examples and under other types of attacks, e.g. attacks with larger perturbations. Meanwhile, regularizers that encourage uncertainty outputs, such as entropy maximization (EntM) and label smoothing (LS) can maintain accuracy on clean examples and improve performance under weak attacks, yet their ability to defend against strong attacks is still in doubt. In this paper, we revisit uncertainty promotion regularizers, including EntM and LS, in the field of adversarial learning. We show that EntM and LS alone provide robustness only under small perturbations. Contrarily, we show that uncertainty promotion regularizers complement AT in a principled manner, consistently improving performance on both clean examples and under various attacks, especially attacks with large perturbations. We further analyze how uncertainty promotion regularizers enhance the performance of AT from the perspective of Jacobian matrices $\nabla_X f(X;\theta)$, and find out that EntM effectively shrinks the norm of Jacobian matrices and hence promotes robustness.

1 INTRODUCTION

Deep neural networks (DNNs) have achieved tremendous success in numerous fields such as image recognition (Russakovsky et al., 2015) and audio recognition (Graves & Jaitly, 2014). However, as pointed out by (Szegedy et al., 2013), DNNs are vulnerable to *adversarial attacks*, where slightly perturbed *adversarial examples* can easily fool DNN classifiers. The ubiquitous existence of adversarial examples (Kurakin et al., 2016) casts doubts on real-world DNN applications, especially those at high stake, such as access control. Therefore, many techniques are proposed aiming to enhance the robustness of DNNs to adversarial attacks (Papernot et al., 2016; Kannan et al., 2018).

Regarding defenses to adversarial attacks, adversarial training (AT) (Goodfellow et al., 2014; Madry et al., 2017) is commonly recognized as the most effective defense. However, it illustrates poor performance on clean examples and under attacks stronger than what they are trained on (Song et al., 2018). Recent works (Rice et al., 2020) attribute such shortcomings to overfitting, but solutions, or even mitigation to them remain open problems. Meanwhile, many regularization techniques are proposed to improve robustness, among which two closely related regularizers, entropy maximization (EntM) and label smoothing (LS) show performance improvements under *weak* attacks (Pang et al., 2019; Shafahi et al., 2019) without compromising accuracy on clean examples. However, as stated by (Uesato et al., 2018; Athalye et al., 2018), strong and various kinds of attacks should be used to better approximate the *adversarial risk* of a defense. Therefore, it remains doubtful how they perform under stronger attacks *by themselves* and how their adversarial risk is.

One appealing property of both EntM and LS is that they both penalize over-confident predictions and promote prediction uncertainty (Pereyra et al., 2017; Szegedy et al., 2016). Therefore, both of them have been used as effective regularizers that mitigate overfitting in multiple applications (Müller et al., 2019). However, it remains unclear whether EntM and LS can effectively regularize AT, where many other regularizers are ineffective (Rice et al., 2020). Therefore, in this paper, we perform an extensive empirical study on uncertainty promotion regularizers, i.e. entropy maximization and label smoothing, in the domain of adversarial machine learning. We carry out experiments on both regularizers, with and without AT, on multiple datasets and under various adversarial set-

tings. We found out that, although neither EntM and LS are able to provide consistent robustness *by themselves*, both regularizers complement AT and improve its performances consistently. The improvement is most evident under attacks with larger perturbations (e.g. 9% improvement under perturbation $\varepsilon = 16/255$ for models trained with $8/255$ AT. See Table 1 and 3). In addition, we investigate the underlying mechanisms about how EntM and LS complement AT, and attribute the improvements to the shrunken norm of Jacobian matrix $\|\nabla_X f(X;\theta)\|$ ($\sim$10 times. See Sect. 6), which indicates better numerical stability and hence better adversarial robustness than AT.

To summarize, we make the following contributions:

1. We carry out an extensive empirical study about whether uncertainty promotion regularizers, i.e. entropy maximization (EntM) and label smoothing (LS), provide better robustness, and find out that while neither of them provides consistent robustness under strong attacks *alone*, both techniques serve as effective regularizers that improve the performance of AT *consistently* on multiple datasets, especially under large perturbations.

2. We provide further analysis on uncertainty promotion regularizers from the perspective of Jacobian matrices, and find out that by promoting prediction uncertainty via EntM, the norm of Jacobian matrix $\|\nabla_X f(X;\theta)\|$ is significantly shrunken, leading to better numerical stability and adversarial robustness than AT.

2 Related Work and Discussions

Adversarial Attacks and Defenses. (Szegedy et al., 2013) was the first work pointing out the vulnerability of DNNs to adversarial examples, which was followed by (Goodfellow et al., 2014) who proposed the Fast Gradient Sign (FGSM) for adversarial attacks and adversarial training. Since then, as increasingly strong adversaries (Carlini & Wagner, 2017) are proposed, AT (Madry et al., 2017) is considered as the most effective defense remaining. More recently, (Zhang et al., 2019) propose TRADES, extending AT and showing better robustness than Madry et al. (2017). We refer readers to (Yuan et al., 2019; Biggio & Roli, 2018) for more comprehensive surveys on adversarial attacks and defenses.

However, all AT methods illustrate common drawbacks. Specifically, Rice et al. (2020) shows that AT suffers from severe overfitting that cannot be easily mitigated, which leads to multiple undesirable consequences. For example, AT performs poorly on clean examples, and Song et al. (2018) shows that AT overfits on the adversary it is trained on and performs poorly under other attacks.

Uncertainty Promotion Techniques in Machine Learning. The principle of maximum entropy is widely accepted in not only physics, but also machine learning, such as reinforcement learning (Ziebart et al., 2008; Haarnoja et al., 2018). In supervised learning, uncertainty promotion techniques, including entropy maximization (Pereyra et al., 2017) and label smoothing (Szegedy et al., 2016) act on model outputs and can improve generalization in many applications, such as image classification and language modeling (Pereyra et al., 2017; Müller et al., 2019; Szegedy et al., 2016).

There are only several works that study uncertainty promotion techniques in the field of adversarial machine learning. ADP (Pang et al., 2019) claims that diversity promotion in ensembles can promote robustness, for which entropy maximization is used. Essentially, ADP consists of multiple mutually independent models that in total mimic the behavior of entropy maximization. However, ADP only shows improvements under weak attacks, e.g. PGD with 10 iterations. Shafahi et al. (2019) claims that label smoothing can improve robustness beyond AT *by itself*, yet the claim remains to be further investigated under a wider range of adversaries, e.g. adaptive attacks and black-box attacks. As stated by (Uesato et al., 2018; Athalye et al., 2018) that, one should use strong and various attackers for better approximation of the *adversarial risk* (Uesato et al., 2018), it remains unknown how much robustness EntM or LS *alone* can provide under strong and diverse attacks. Moreover, neither of these works study the relationship between AT and uncertainty promotion, which is an important open problem since many regularizers fail to mitigate the overfitting of AT (Rice et al., 2020).

3 PRELIMINARIES

Notations. We denote a dataset $\mathcal{D} = \{X^{(i)}, y^{(i)}\}_{i=1}^{n}$, where $X^{(i)} \in \mathbb{R}^d$ are input data, $y^{(i)} \in \mathbb{R}^C$ are one-hot vectors denoting class labels. We denote a deep neural network parameterized by θ as $f(X;\theta) : \mathbb{R}^d \to \mathbb{R}^C$, which outputs logits on classes $[C]$[1]. We denote $f_\sigma(X;\theta) = \sigma \circ f(X;\theta)$, the network followed by softmax transforming logits into probabilities. We denote the cross entropy loss as $\mathrm{CE}(\hat{y}, y) = -\sum_{i=1}^{C} y_i \log \hat{y}_i$, the Shannon entropy as $H(p) = -\sum_{i=1}^{C} p_i \log p_i$ and the Kullback-Leibler divergence as $D_{KL}(p\|q) = \sum_{i=1}^{C} p_i \log \frac{p_i}{q_i}$.

Adversarial Attacks and Adversarial Training. Given a data-label pair (X, y) and a neural network $f(X;\theta)$, adversarial attacks aim to craft an adversarial example $X^{(adv)}$, $\|X^{(adv)} - X\| \leq \varepsilon$, so as to fool $f(X;\theta)$. Such goal can be formulated as the problem:

$$X^{(adv)} = \arg\max_{X'} L_{atk}(f_\sigma(X';\theta), y), \text{ subject to} \|X' - X\| \leq \varepsilon. \tag{1}$$

where L_{atk} is some loss function, generally taken as CE. Eqn. 1 can generally be solved via iterative optimization, such as Projected Gradient Descent (PGD) (Madry et al., 2017).

Adversarial Training (AT) is generally considered the most effective defense against adversarial attacks, where the training set consists of both clean examples and adversarial examples, and the following objective is minimized (Goodfellow et al., 2014),

$$\min_\theta \mathbb{E}_{(X,y)\sim\mathcal{D}} \left[\alpha \mathrm{CE}\left(f_\sigma(X;\theta), y\right) + (1-\alpha) \max_{\|X^{(adv)}-X\|\leq\varepsilon} \mathrm{CE}\left(f_\sigma(X^{(adv)};\theta), y\right) \right], \tag{2}$$

where the inner maximization is commonly solved via PGD. We specifically denote AT which uses PGD to solve the inner problem as PAT (Madry et al., 2017). TRADES (Zhang et al., 2019) extends PAT by optimizing Eqn. 3 in similar min-max styles, leading to better robustness than PAT.

$$\min_\theta \mathbb{E}_{(X,y)\sim\mathcal{D}} \left[\mathrm{CE}(f_\sigma(X;\theta), y) + \beta \max_{\|X^{(adv)}-X\|\leq\varepsilon} D_{KL}\left(f_\sigma(X^{(adv)};\theta) \| f_\sigma(X;\theta)\right) \right]. \tag{3}$$

4 METHODOLOGY

4.1 ENTROPY MAXIMIZATION

Given an example (X, y) and a neural network $f(X;\theta)$, the proposed entropy maximization (EntM) minimizes the cross entropy loss, while maximizing the Shannon entropy of the output probability.

$$L_{entm}(X, y) = \mathrm{CE}\left(f_\sigma(X;\theta), y\right) - \lambda H\left(f_\sigma(X;\theta)\right), \tag{4}$$

where λ is a hyperparameter controlling the strength of entropy maximization. For normal training, we minimize over $\mathbb{E}_{(X,y)\sim\mathcal{D}}[L_{entm}(X, y)]$; for AT, such as PAT and TRADES, we replace CE with L_{entm} in Eqn. 2, which for PAT yields Eqn. 5, and similarly for TRADES:

$$\min_\theta \mathbb{E}_{(X,y)\sim\mathcal{D}} \left[\alpha L_{entm}\left(f_\sigma(X;\theta), y\right) + (1-\alpha) \max_{\|X^{(adv)}-X\|\leq\varepsilon} L_{entm}\left(f_\sigma(X^{(adv)};\theta), y\right) \right], \tag{5}$$

The entropy maximization term penalizes for over-confident outputs and encourages uncertain predictions, which is different from CE encouraging one-hot outputs. Such a formulation is also seen in (Pereyra et al., 2017; Dubey et al., 2018) in general deep learning and fine-grained classification.

4.2 CONNECTION WITH LABEL SMOOTHING

Label smoothing is also a widely used technique that prevents assigning over-confident predictions. Given a data-label pair (X, y), and denote the uniform distribution over C classes as u_C, the objective of label smoothing can be formulated as

$$y_{smooth} = y - \gamma(y - u_C), L_{smooth}(X, y) = \mathrm{CE}\left((f_\sigma(X;\theta), y_{smooth}\right). \tag{6}$$

[1] We omit the parameters θ and denote the network as $f(X)$ when discussions are not related to θ.

Label smoothing and entropy maximization are intrinsically similar. Specifically, both label smoothing and entropy maximization penalize over-confident outputs by:

$$L_{smooth}(X, y) = (1-\gamma)\,\mathrm{CE}(f_\sigma(X;\theta), y) + \gamma D_{KL}(u_C \| f_\sigma(X;\theta)) + \gamma \log C. \tag{7}$$

$$L_{entm}(X, y) = \mathrm{CE}(f_\sigma(X;\theta), y) + \lambda D_{KL}(f_\sigma(X;\theta) \| u_C) - \lambda \log C. \tag{8}$$

Therefore EntM and LS are connected, with differences in the asymmetric $D_{KL}(f_\sigma(X;\theta)\|u_C)$ and $D_{KL}(u_C\|f_\sigma(X;\theta))$. In our paper, we carry out experiments on LS and EntM for comparison.

5 Quantitative Experiments

5.1 Experimental Settings and Results

Datasets and Models We utilize four commonly used datasets for evaluation, CIFAR-10, CIFAR-100, SVHN and MNIST. We train ResNet18, a common selection in adversarial training (Madry et al., 2017) for CIFAR-10, SVHN and CIFAR-100, and a four-layer CNN for MNIST. Details about training settings and architectures can be found in the Appendix.

Comparison Models We study the robustness of the following models without adversarial training.

- Normal models trained using standard cross entropy. We denote them as **Normal**.
- **ADP** (Pang et al., 2019), where they built ensembles of models, regularized by maximizing their ensemble diversity. Entropy maximization is involved in the ensemble diversity term. We use 3 models as the ensemble, and take the recommended parameters $(2, 0.5)$.
- Models trained with **EntM** in Eqn. 4. We set $\lambda = 2$ for all datasets following ADP who also set the entropy term to 2.
- Models trained with label smoothing (**LS**). We choose γ such that the non-maximal predictions are the same as EntM on each dataset, i.e. $\gamma = 0.74$ for CIFAR-10 and SVHN, and $\gamma = 0.84$ for CIFAR-100.

We also study the robustness of the following models with adversarial training. All adversaries are taken as L_∞ adversary with $\varepsilon = 8/255$, step size $2/255$ with 7 steps for CIFAR-10, CIFAR-100 and SVHN, and $\varepsilon = 48/255$, step size $6/255$ with 10 steps for MNIST.

- AT (Eqn. 2) with PGD adversary, (**PAT**). We take $\alpha = 0.5$ as in (Goodfellow et al., 2014).
- PAT with EntM objective (Eqn. 5), **PAT-EntM**. We set identical λ as in EntM..
- PAT with label smoothing (Eqn. 6), **PAT-LS**. We set identical γ values as in LS.
- **TRADES** (Zhang et al., 2019), which shows better robustness than PAT. We take $\beta = 3$. [2]

Threat models. Without explicit mentioning, we focus on untargeted L_∞ adversaries. We consider PGD adversaries with CE objective (referred to PGD and FGSM), and also CW adversaries (Carlini & Wagner, 2017), i.e. adversaries using CW objective and optimized by PGD[3]. We consider both **white** and **black-box** settings. In black-box settings, adversarial examples are crafted on a proxy model trained on identical data and then transferred to the target model (Papernot et al., 2017).

We show test accuracy under various attacks on CIFAR-10, CIFAR-100, SVHN and MNIST in Table 1, 2, 3 and 9[4]. We use FGSMk to denote FGSM with $\varepsilon = k/255$, PGD$p-k$ as p-step PGD attacks with $\varepsilon = k/255$, step size $k/2550$, and CW$p-k$ as similar to PGD$p-k$ except for the attack objective. We adopt random initialization with Gaussian $X' = X + N(0, 0.005)$ with 5 restarts for all attacks. For black-box attacks, adversarial examples are crafted on a Normal model for defenses without AT, and on a PAT model for those with AT. Best accuracies higher than random are bolded.

[2] We also did experiments on TRADES-EntM, i.e. TRADES trained with entropy maximization objective. The results are shown in Table 11 and 12 in the Appendix.

[3] The C&W adversary is implemented and carried out exactly as (Zhang et al., 2020).

[4] Results on MNIST are shown in the Appendix. We also show results on PGD20 in the Appendix.

CIFAR-10 Mode	Attacks	Normal	Without AT			With AT			
			EntM	LS	ADP	PAT	TRADES	PAT-EntM	PAT-LS
White-Box	Clean	94.78	94.71	95.15	**95.72**	86.47	84.01	87.87	**88.31**
	FGSM4	37.05	72.37	**74**	69.5	69.21	70.33	**72.96**	**72.95**
	PGD10-4	3.27	*58.45*	***66.07***	*42.8*	68.33	68.72	71.26	**71.48**
	PGD10-8	0	*37.49*	***46.12***	*21.38*	48.87	51.35	**53.89**	53.22
	PGD10-16	0	17.06	**24.79**	6.25	19.63	25.77	**33.65**	31.17
	PGD40-4	0	21.12	**24.6**	12.15	67.51	67.4	**69.63**	69.44
	PGD40-8	0	5.01	6.26	1.94	43.03	**46.74**	45.95	44.79
	PGD40-16	0	0.7	0.93	0.13	10.26	15.27	**19.56**	18.3
	CW40-4	0	22.76	**24.8**	-	67.04	66.31	68.3	**68.58**
	CW40-8	0	6.7	9.28	-	43.63	**45.78**	44.52	43.75
	CW40-16	0	1.16	2.35	-	10.66	14.47	**17.79**	17.09
Black-Box	PGD10-4	27.5	**35.84**	32.24	31.79	76.88	75.52	**79.32**	79.24
	PGD10-8	7.57	**13.26**	10.2	10.12	63.9	64.8	**65.82**	65.76

Table 1: Performance under various attacks on CIFAR-10 (%). 0 denotes $< 0.1\%$. Italics indicate white-box accuracies higher than corresponding black-box ones.

CIFAR-100 Mode	Attacks	Normal	Without AT			With AT			
			EntM	LS	ADP	PAT	TRADES	PAT-EntM	PAT-LS
White-Box	Clean	75.66	77.17	77.60	**80.04**	59.65	54.63	62.53	**62.83**
	FGSM4	12.73	28.29	29.8	**31.14**	38.86	37.94	**44.37**	43.2
	PGD10-4	0.97	9.1	**9.91**	6.15	37.76	37.61	**43.43**	42.39
	PGD10-8	0	**3.32**	**3.35**	1.3	22.41	24.77	**29.09**	27.13
	PGD10-16	0	0.7	1	0	7.47	10.28	**13.18**	11.21
	PGD40-4	0	1.08	1.35	0.87	36.55	36.45	**42.45**	41.08
	PGD40-8	0	0.1	0	0	19.62	22.6	**26.1**	24.05
	PGD40-16	0	0	0	0	4.73	7.26	**8.22**	6.69
	CW40-4	0	0.4	0.5	-	36.09	34.29	**38.5**	38.02
	CW40-8	0	0	0	-	19.33	20.74	**22.17**	21.02
	CW40-16	0	0	0	-	5.1	6.01	**6.17**	5.4
Black-Box	PGD10-4	13.77	18.07	18.44	**21.36**	49.4	46.76	52.25	**52.97**
	PGD10-8	3.65	5.45	5.6	**7.07**	38.84	38.55	**41.48**	41.44

Table 2: Performance under various attacks on CIFAR-100 (%).

5.2 How much do Uncertainty Promotion regularizers improve robustness?

5.2.1 Without Adversarial Training

We first analyze the case where no adversarial training is used, namely, EntM, ADP and LS, whose robustness under diverse and strong attacks is under question. We make the following findings.

- Under attacks, EntM and LS perform better than ADP in CIFAR-10 and CIFAR-100, and in SVHN, LS performs better than ADP, while EntM performs similarly as ADP. Therefore we focus our analysis on EntM and LS instead of ADP.
- **EntM and LS show gradient obfuscation under weak attacks.** On CIFAR-10 and SVHN, white-box PGD10 attacks succeed less often than black-box ones (See Table 1 and 3, White-Box and Black-Box PGD10), which is a clear indication of *gradient obfuscation* (Athalye et al., 2018), i.e. gradient-based attacks with few steps perform even worse than gradient-free attacks because gradients around a data point are made useless by the model. Gradient obfuscation on EntM and LS leads us to use adversaries with more steps to better approximate their *true* robustness, as multi-step adversaries are more likely to escape from the area where gradient obfuscation happens and find adversarial examples.

SVHN Mode	Attacks	Normal	Without AT			With AT			
			EntM	LS	ADP	PAT	TRADES	PAT-EntM	PAT-LS
White-Box	Clean	97.04	97.18	97.31	**97.58**	94	93.28	**94.08**	**94.08**
	FGSM4	65.74	85.39	**85.75**	83.55	82.99	**84.26**	83.21	83.04
	PGD10-4	27.54	*72.99*	***79.86***	*70.76*	79.72	**80.41**	80.11	79.39
	PGD10-8	4.73	48.47	***59.13***	*49.91*	61.71	**64.95**	63.88	62.6
	PGD10-16	0	21.61	**31.97**	25.13	29.33	36.27	**38.85**	35.77
	PGD40-4	8.37	40.85	**44.53**	42.73	77.71	77.96	**78.3**	77.06
	PGD40-8	0.36	10.27	12.4	**13.62**	52.76	**57.02**	54.65	52.14
	PGD40-16	0	1.15	1.9	2.25	14.18	17.96	**23.8**	17.58
Black-Box	PGD10-4	66.07	**70.47**	69.76	67.83	83.69	83.78	83.85	**84.08**
	PGD10-8	43.7	**49.77**	48.25	46.53	68.88	69.4	69.03	**69.48**

Table 3: Performance under various attacks on SVHN (%). Italics indicate white-box accuracies higher than corresponding black-box ones.

- **EntM and LS improve robustness only under small perturbations.** We carry out evaluations on PGD40. It can be shown that under PGD40-8 and 16, EntM, LS and ADP fail to perform better than random guessing on all datasets, and improvements over random can only be seen under PGD40-4 on CIFAR-10 and SVHN (Table 1 and 3). Therefore, the claims by (Pang et al., 2019; Shafahi et al., 2019) that ADP and LS improve robustness are conditional, and that EntM, LS and ADP are only robust under small perturbations.

5.2.2 With Adversarial Training

We then study uncertainty promotion regularizers in conjunction with AT and make the following findings.

- PAT-EntM and PAT-LS outperform PAT on clean examples by 1% on CIFAR-10, 3% on CIFAR-100, and under strong attacks like PGD40, outperform PAT by 2-9% on CIFAR-10, and 3-6% on CIFAR-100. See Clean and PGD40 in Table 1, 3, 2.
- PAT-EntM achieves generally similar or better performance than its counterpart PAT-LS, e.g. on CIFAR-10 and CIFAR-100, PAT-EntM achieves 1% better adversarial accuracy, while PAT-LS achieves <1% better accuracy on clean examples, see Table 1 and 2. Therefore for the rest of the paper we primarily focus on PAT-EntM.
- Robustness improvements are most evident under large perturbations. For example, accuracies under PGD40-16 improved by 9% on CIFAR-10 and SVHN from PAT to PAT-EntM, see Table 1 and 3, which is exactly the opposite from where AT is not used.
- In terms of accuracy under attacks, PAT-EntM outperforms stronger baseline TRADES by over 3% on CIFAR-10 and CIFAR-100, and achieve similar performances as TRADES on SVHN, further showing the effectiveness of uncertainty promotion regularizers.
- We also tested all AT defenses under CW on CIFAR-10 and CIFAR-100, see Table 1 and 2. Results show that PAT-EntM shows better robustness under CW attacks than PAT (as much as 7% on CIFAR-10 and 3% on CIFAR-100). Also, PAT-EntM shows better robustness than TRADES (except for CIFAR-10, CW40-8). The results under a different kind of adversary further demonstrates the robustness improvement provided by EntM.

Following the suggestions of (Athalye et al., 2018), we perform the following sanity checks to make sure PAT-EntM is not only disabling weak attacks like EntM and LS, and better approximate and evaluate its adversarial risk.

Perturbation-Accuracy Curve. We expand perturbations to test whether the robust accuracy monotonically decreases, and whether sufficiently large perturbations reduce accuracy to 0. We utilize L_∞ PGD with $\varepsilon = k/255$, step size $2/255$ and k iterations for $k \in [10, 150]$, on PAT, PAT-EntM and TRADES models, on CIFAR-10 and CIFAR-100. We show the results in Fig. 1. It can be shown that in both datasets and under all ε, PAT-EntM outperforms PAT and TRADES. Moreover,

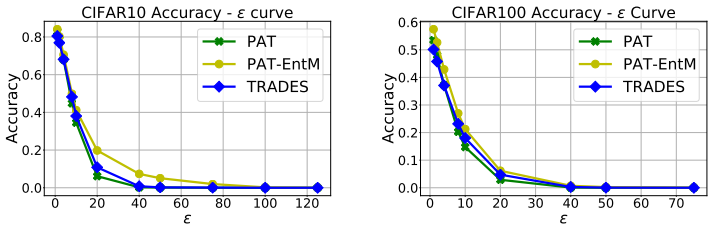

(a) CIFAR-10 (b) CIFAR-100

Figure 1: Accuracy-ε curve on CIFAR-10 and CIFAR-100. x-axis values denote pixel changes.

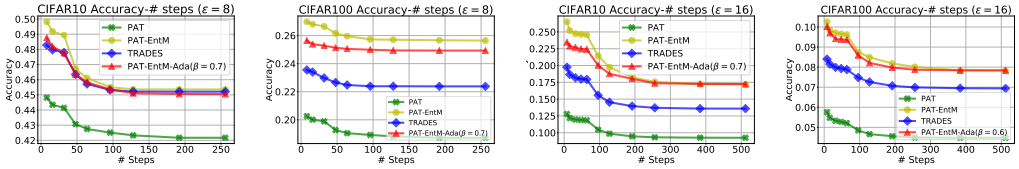

(a) CIFAR-10, $\varepsilon = 8$ (b) CIFAR-100, $\varepsilon = 8$ (c) CIFAR-10, $\varepsilon = 16$ (d) CIFAR-100, $\varepsilon = 16$

Figure 2: Accuracy-# step curve on CIFAR-10 and CIFAR-100. $\varepsilon = 8/255, 16/255$

under sufficiently large ε, all accuracies drop to 0, which is another evidence that PAT-EntM is improving robustness rather than obfuscating gradients.

Attacks with more iterations.

We perform attacks with fixed ε and more iterations to make sure attacks converge, and to reliably evaluate the robustness of PAT-EntM. We take $\varepsilon = 8/255, 16/255$, with # steps $k \in [8, 256]$, step size $\max(1/510, 2\varepsilon/k)$ on CIFAR-10 and CIFAR-100.

We show the results in Fig. 2. It can be shown that more iterations lead to stronger attacks, and when the attacks converge at 200 steps, PAT-EntM still achieves consistent performance increase (over 4% on both CIFAR-10 and CIFAR-100). Moreover, PAT-EntM performs better than TRADES in all cases, which further endorses the robustness improvement provided by EntM.

Adaptive Attacks. We perform adaptive attacks on PAT-EntM. Due to its connection with label smoothing, we leverage CE with smoothed labels in Eqn. 6 as the loss function L_{atk} in Eqn. 1. We search for the best parameter γ for each attack from $[0, 1]$ at an interval of 0.1. We consider $\varepsilon = 8/255, 16/255$ on CIFAR-10 and CIFAR-100, and plot corresponding curves also in Fig. 2.

It can be shown in Fig. 2 that with properly selected smooth parameter γ, adaptive attacks are able to reduce robust accuracies compared to non-adaptive ones. However, even under strong adaptive attacks, we can still see performance gain of PAT-EntM over PAT (e.g. 7% on CIFAR-10 and 4% on CIFAR-100, $\varepsilon = 16/255$) and in most cases over TRADES, except for CIFAR-10, $\varepsilon = 8/255$, where PAT-EntM is <0.5% less robust than TRADES under strong adaptive attacks (45.05% and 45.21%). However, PAT-EntM is 3.8% more accurate on clean examples than TRADES, and therefore we still consider PAT-EntM more competitive than TRADES.

5.3 Hyperparameter Analysis

We vary the hyperparameter λ in Eqn. 4 and 5 to see how the uncertainty level λ influences accuraries on both clean and adversarial examples. We vary $\lambda \in [0, 10]$ on CIFAR-10 and CIFAR-100.

We plot the accuracies on clean examples and under PGD40-8 in Fig. 3. The results show that on both datasets, accuracies on both clean and adversarial examples simultaneously increase with λ before $\lambda = 5$. This is an appealing property and contrary to the belief that accuracy and robustness are at odds with each other (Zhang et al., 2019; Tsipras et al., 2018).

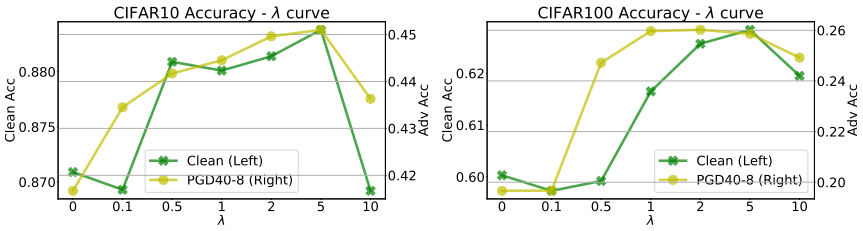

(a) CIFAR-10 (b) CIFAR-100

Figure 3: Hyperparameter Analysis for λ.

We also observe in FIg. 3 that on both datasets, $\lambda = 2$ and $\lambda = 5$ achieve similar performances in terms of both accuracy and robustness (within 0.5%), which shows that EntM is not highly sensitive to hyperparameters.

6 How Uncertainty Promotion Works - Further Analysis

In this section we dig deeper into how uncertainty promotion works, which may bring deeper insights towards more robust algorithms. For brevity, in this section, we use $f(X)$ as a shorthand for $f(X;\theta)$ for brevity. We focus on the first-order approximation of $f(X)$,

$$f(X') \approx f(X) + \nabla_X f(X)^T (X' - X) \tag{9}$$

If the approximation holds well locally, we have the following inequality:

$$\|f(X') - f(X)\|_2 \approx \|\nabla_X f(X)^T (X' - X)\|_2 \leq \|\nabla_X f(X)\|_2 \|X' - X\|_2, \tag{10}$$

$$\|\nabla_X f(X)\|_2 \geq \frac{\|f(X) - f(X')\|_2}{\|X' - X\|_2} \tag{11}$$

where $\|\nabla_X f(X)\|_2$ is the spectral norm (also the largest singular value) of the Jacobian matrix. It can be shown by Eqn. 11 that $\|\nabla_X f(X)\|_2$ *locally* upper bounds the local Lipschitz constant of $f(X)$ at point X (denoted as $l_{f,X}$). Denoting $M_{f,X} = f(X)_y - \max_{i \neq y} f(X)_i$ as the decision margin, Tsuzuku et al. (2018) shows the relationship between $M_{f,X}$, Lipschitzness, and robustness.

Theorem 1. *Denote the global Lipschitz constant of $f(X;\theta)$ as l_f. The following holds for any point X, and any perturbation δ.*

$$M_{f,X} \geq \sqrt{2}\|\delta\|_2 l_f \Rightarrow M_{f,X+\delta} \geq 0. \tag{12}$$

In practice, we replace l_f, the global Lipschitz constant with $l_{f,X}$ at each point X, which is upper bounded by $\|\nabla_X f(X)\|_2$, and compute $\frac{M_{f,X}}{\|\nabla_X f(X)\|_2}$. According to Theorem 1, $\frac{M_{f,X}}{\|\nabla_X f(X)\|_2}$ locally shows how much perturbation is allowed without flipping predictions. However, considering the fact that $f(X)$ is non-linear, we define another term $Q_f(X', X)$ describing how much $f(X;\theta)$ deviates from the linear approximation, to account for cases where Eqn. 9 approximates poorly.

$$Q_f(X', X) = \frac{\|f(X') - f(X) - \nabla_X f(X)^T (X' - X)\|_2}{\|\nabla_X f(X)^T (X' - X)\|_2}, \|X' - X\|_2 \leq \varepsilon. \tag{13}$$

We sample 2,000 test samples (X, y) from CIFAR-10, and study the relationship among *normalized margin* $\frac{M_{f,X}}{\|\nabla_X f(X)\|_2}$, *non-linearity* $Q_f(X', X)$, and *robustness*. We use L_2 adversaries in correspondence with Theorem 1. We list related results in Table 4. With EntM, $\|\nabla_X f(X)\|_2$ is shrunken by over 10 times regardless whether AT is used, leading to a 4-time increase of normalized margin in both EntM and PAT-EntM. However, while EntM alone achieves high regularized margin, it also massively compromises *local linearity* compared to Normal, as shown by the high $Q_f(X^{(adv)}, X)$. Therefore, the area where the linear approximation in Eqn. 9-11 holds is limited, thereby unable to

Models	Normal	EntM	PAT	PAT-EntM
$M_{f,X}$	10.55	1.3054	6.12	1.12
$\|\nabla_X f(X)\|_2$	72.26	3.44	10.69	0.84
$\frac{M_{f,X}}{\|\nabla_X f(X)\|_2}$	0.1919	2.8132	0.6398	2.9913
Accuracy (PGD20-0.5)	0.0029	0.166	0.5909	0.6142
$Q_f(X^{(adv)}, X)$	4.4	52.51	4.59	5.36
Correlation$\left(\frac{M_{f,X}}{\|\nabla_X f(X)\|_2}, \|X^{(adv)} - X\|_2\right)$	0.8327	0.4794	0.8216	0.8131

Table 4: Analysis of margin $M_{f,X}$, Jacobian matrix $\nabla_X f(X;\theta)$ and non-linearity $Q_f(X^{(adv)}, X)$.

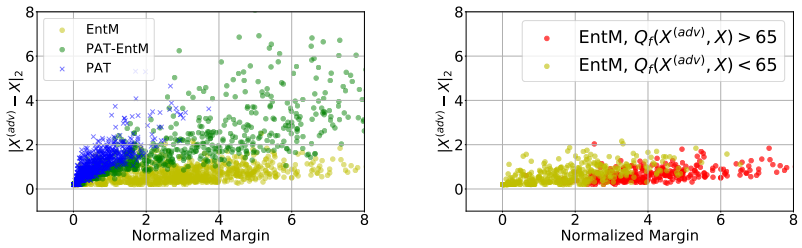

(a) EntM, PAT, PAT-EntM (b) EntM, High and low $Q_f(X^{(adv)}, X)$

Figure 4: Relationship between normalized margin and distortion for EntM, PAT and PAT-EntM.

guarantee robustness. By contrast, PAT-EntM only worsens local linearity slightly compared to PAT, and therefore the enlarged normalized margin contributes to better robustness.

We further show that normalized margin, along with local linearity explains the improvement. We leverage an infinite L_2 adversary to attack each example X until $X^{(adv)}$ causes misclassification. We then compute the distortions $\|X^{(adv)} - X\|_2$, and study the relationship between distortions and normalized margins. A more robust model should require a larger distortion to successfully attack.

First, we plot the normalized margins and distortions in Fig 4(a), and show their Pearson correlations in Table 4. It can be shown that on Normal, PAT, PAT-EntM, the correlation is much higher than that on EntM. It is also shown in Fig. 4(a) that although EntM show similar normalized margins as PAT-EntM, the distortions required are still small. On the contrary, the larger normalized margins of PAT-EntM lead to larger distortions and hence better robustness than PAT. We further separate points with $Q_f(X^{(adv)}, X) > 65$, which is the top 40% in terms of $Q_f(X^{(adv)}, X)$, and plot them separately in Fig. 4(b). It can be shown that samples with higher local non-linearity show higher normalized margins as PAT-EntM, but no higher distortion and hence no better robustness. All results show that normalized margins, combined with local linearity, explains robustness.

7 Conclusion

In this paper, we revisit uncertainty promotion regularizers in the field of adversarial learning. We find out that uncertainty promotion regularizers alone are causing gradient obfuscation that may improve performance under weak attacks, and that they alone only provide inconsistent robustness against small perturbations. Contrarily, our extensive experiments demonstrate that uncertainty promotion regularizers augment AT, improving accuracy on clean examples and enhancing robustness, especially under large perturbations. We further demonstrate that both good local linearity and shrunken norm of Jacobian matrices contribute to better robustness shown by PAT-EntM than PAT.

We hope that this paper would again underscore the necessity to evaluate under strong attacks, and raise attention to further insights about why uncertainty promotion regularizers work. We consider theoretical investigations of why they work well alongside AT as an important future work.

REFERENCES

Anish Athalye, Nicholas Carlini, and David Wagner. Obfuscated gradients give a false sense of security: Circumventing defenses to adversarial examples. In *International Conference on Machine Learning*, pp. 274–283, 2018.

Battista Biggio and Fabio Roli. Wild patterns: Ten years after the rise of adversarial machine learning. *Pattern Recognition*, 84:317–331, 2018.

Nicholas Carlini and David Wagner. Towards evaluating the robustness of neural networks. In *2017 ieee symposium on security and privacy (sp)*, pp. 39–57. IEEE, 2017.

Abhimanyu Dubey, Otkrist Gupta, Ramesh Raskar, and Nikhil Naik. Maximum-entropy fine grained classification. In *Advances in Neural Information Processing Systems*, pp. 637–647, 2018.

Ian J Goodfellow, Jonathon Shlens, and Christian Szegedy. Explaining and harnessing adversarial examples. *arXiv preprint arXiv:1412.6572*, 2014.

Alex Graves and Navdeep Jaitly. Towards end-to-end speech recognition with recurrent neural networks. In *International Conference on Machine Learning*, pp. 1764–1772, 2014.

Tuomas Haarnoja, Aurick Zhou, Pieter Abbeel, and Sergey Levine. Soft actor-critic: Off-policy maximum entropy deep reinforcement learning with a stochastic actor. *arXiv preprint arXiv:1801.01290*, 2018.

Harini Kannan, Alexey Kurakin, and Ian Goodfellow. Adversarial logit pairing. *arXiv preprint arXiv:1803.06373*, 2018.

Alexey Kurakin, Ian Goodfellow, and Samy Bengio. Adversarial examples in the physical world. *arXiv preprint arXiv:1607.02533*, 2016.

Aleksander Madry, Aleksandar Makelov, Ludwig Schmidt, Dimitris Tsipras, and Adrian Vladu. Towards deep learning models resistant to adversarial attacks. *arXiv preprint arXiv:1706.06083*, 2017.

Rafael Müller, Simon Kornblith, and Geoffrey E Hinton. When does label smoothing help? In *Advances in Neural Information Processing Systems*, pp. 4694–4703, 2019.

Tianyu Pang, Kun Xu, Chao Du, Ning Chen, and Jun Zhu. Improving adversarial robustness via promoting ensemble diversity. In *International Conference on Machine Learning*, pp. 4970–4979, 2019.

Nicolas Papernot, Patrick McDaniel, Xi Wu, Somesh Jha, and Ananthram Swami. Distillation as a defense to adversarial perturbations against deep neural networks. In *2016 IEEE Symposium on Security and Privacy (SP)*, pp. 582–597. IEEE, 2016.

Nicolas Papernot, Patrick McDaniel, Ian Goodfellow, Somesh Jha, Z Berkay Celik, and Ananthram Swami. Practical black-box attacks against machine learning. In *Proceedings of the 2017 ACM on Asia conference on computer and communications security*, pp. 506–519, 2017.

Gabriel Pereyra, George Tucker, Jan Chorowski, Łukasz Kaiser, and Geoffrey Hinton. Regularizing neural networks by penalizing confident output distributions. *arXiv preprint arXiv:1701.06548*, 2017.

Leslie Rice, Eric Wong, and J Zico Kolter. Overfitting in adversarially robust deep learning. *arXiv preprint arXiv:2002.11569*, 2020.

Olga Russakovsky, Jia Deng, Hao Su, Jonathan Krause, Sanjeev Satheesh, Sean Ma, Zhiheng Huang, Andrej Karpathy, Aditya Khosla, Michael Bernstein, et al. Imagenet large scale visual recognition challenge. *International journal of computer vision*, 115(3):211–252, 2015.

Ali Shafahi, Amin Ghiasi, Furong Huang, and Tom Goldstein. Label smoothing and logit squeezing: A replacement for adversarial training? *arXiv preprint arXiv:1910.11585*, 2019.

Chuanbiao Song, Kun He, Liwei Wang, and John E Hopcroft. Improving the generalization of adversarial training with domain adaptation. *arXiv preprint arXiv:1810.00740*, 2018.

Christian Szegedy, Wojciech Zaremba, Ilya Sutskever, Joan Bruna, Dumitru Erhan, Ian Goodfellow, and Rob Fergus. Intriguing properties of neural networks. *arXiv preprint arXiv:1312.6199*, 2013.

Christian Szegedy, Vincent Vanhoucke, Sergey Ioffe, Jon Shlens, and Zbigniew Wojna. Rethinking the inception architecture for computer vision. In *Proceedings of the IEEE conference on computer vision and pattern recognition*, pp. 2818–2826, 2016.

Dimitris Tsipras, Shibani Santurkar, Logan Engstrom, Alexander Turner, and Aleksander Madry. Robustness may be at odds with accuracy. *arXiv preprint arXiv:1805.12152*, 2018.

Yusuke Tsuzuku, Issei Sato, and Masashi Sugiyama. Lipschitz-margin training: Scalable certification of perturbation invariance for deep neural networks. In *Advances in neural information processing systems*, pp. 6541–6550, 2018.

Jonathan Uesato, Brendan O'Donoghue, Pushmeet Kohli, and Aaron Oord. Adversarial risk and the dangers of evaluating against weak attacks. In *International Conference on Machine Learning*, pp. 5025–5034, 2018.

Xiaoyong Yuan, Pan He, Qile Zhu, and Xiaolin Li. Adversarial examples: Attacks and defenses for deep learning. *IEEE transactions on neural networks and learning systems*, 30(9):2805–2824, 2019.

Hongyang Zhang, Yaodong Yu, Jiantao Jiao, Eric Xing, Laurent El Ghaoui, and Michael Jordan. Theoretically principled trade-off between robustness and accuracy. In *International Conference on Machine Learning*, pp. 7472–7482, 2019.

Jingfeng Zhang, Xilie Xu, Bo Han, Gang Niu, Lizhen Cui, Masashi Sugiyama, and Mohan Kankanhalli. Attacks which do not kill training make adversarial learning stronger. *arXiv preprint arXiv:2002.11242*, 2020.

Brian D Ziebart, Andrew L Maas, J Andrew Bagnell, and Anind K Dey. Maximum entropy inverse reinforcement learning. In *Aaai*, volume 8, pp. 1433–1438. Chicago, IL, USA, 2008.

A Detailed Experimental Settings

A.1 Architectures

We train ResNet18 for CIFAR-10, CIFAR-100 and SVHN. We use the same architecture of ResNet18 as in TRADES[5]. The input size for ResNet18 is $32 \times 32 \times 3$.

We train a four-layer CNN for MNIST. The detailed architecture is:

- Input: $28 \times 28 \times 1$ grayscale images.
- 5x5 convolution with stride 5 and 10 filters. ReLU activation.
- Max pooling with stride 2.
- 5x5 convolution with stride 5 and 20 filters. ReLU activation.
- Max pooling with stride 2.
- Flatten.
- FC layer with input shape 320 and output 10. ReLU activation.
- FC layer with input shape 50 and output shape 10.

Settings/Models	Four-layer	ResNet18, without AT	ResNet18, with AT
Input Scale		$[0, 1]$	
Input Size	$28 \times 28 \times 1$	$32 \times 32 \times 3$	$32 \times 32 \times 3$
Total Training Epochs	40	200	120
Weight Decay	10^{-4}	10^{-4}	10^{-4}
Optimizer		SGD with momentum 0.9	
Initial Learning Rate	0.01	0.1	0.1
Learning Rate Decay Rate	0.1	0.1	0.1
Learning Rate Decay Epoch	20	$[100, 150]$	$[60, 84, 100]$
Early Stopping	No	No	No
Batch Size	128	64	64

Table 5: Training Settings

A.2 Training Parameter Settings

We list all training settings in Table 5. For each quantitative result, we train 3 models, and each PGD is repeated 3 times for average.

For datasets, we perform standard data augmentation techniques, including random cropping and random horizontal flipping (on CIFAR-10 and CIFAR-100).

B Full Experimental Results

CIFAR-10	Attacks	Normal	Without AT			With AT			
Mode			EntM	ADP	LS	PAT	PAT-EntM	PAT-LS	TRADES
White-Box	Clean	94.78	94.71	**95.72**	95.15	86.47	87.87	**88.31**	84.01
	FGSM4	37.05	72.37	69.5	**74**	70.33	**72.96**	**72.95**	69.21
	PGD10-4	3.27	*58.45*	*42.8*	***66.07***	68.33	71.26	**71.48**	68.72
	PGD10-8	0	*37.49*	*21.38*	***46.17***	48.87	**53.89**	53.22	51.35
	PGD10-16	0	17.06	6.25	**24.79**	19.63	**33.65**	31.17	25.77
	PGD20-4	0.31	*36.73*	22.38	***47.86***	67.89	**70.1**	69.88	67.58
	PGD20-8	0	*14.59*	*5.8*	***23.11***	44.61	**48.72**	47.4	47.82
	PGD20-16	0	3.86	0.82	7.95	12.76	**24.79**	22.73	18.27
	PGD40-4	0	21.12	12.15	**24.6**	67.51	**69.63**	69.44	67.4
	PGD40-8	0	5.01	1.94	6.26	43.03	45.95	44.79	**46.74**
	PGD40-16	0	0.7	0.13	0.93	10.26	**19.56**	18.3	15.27
Black-Box	PGD10-4	27.5	**35.84**	31.79	32.24	76.88	**79.32**	79.24	75.52
	PGD10-8	7.57	**13.26**	10.12	10.2	63.9	**65.82**	65.76	64.8
	PGD20-4	19.73	**28.53**	24.78	26.75	76.73	**78.67**	**78.69**	74.84
	PGD20-8	3.12	**7.43**	5.36	6.46	62.24	**64.44**	64	63.65

Table 6: Performance under various attacks on CIFAR-10 (%). 0 denotes $< 0.1\%$. Italics indicate white-box accuracies higher than corresponding black-box ones.

We show full experimental results in 6, 7, 8 and 9. Although in MNIST, the improvement is less significant (1% or below), and TRADES significantly outperforms both PAT and PAT-EntM, PAT-EntM still achieves improvement over AT in terms of robustness under various attacks.

C Gradient Obfuscation of LS and EntM without AT

In this section we present more evidence regarding gradient obfuscation.

[5] https://github.com/yaodongyu/TRADES/blob/master/models/resnet.py

CIFAR-100 Mode	Attacks	Normal	Without AT			With AT			
			EntM	ADP	LS	PAT	PAT-EntM	PAT-LS	TRADES
White-Box	Clean	75.66	77.17	**80.04**	77.60	59.65	62.53	**62.83**	54.63
	FGSM4	12.73	29.8	28.29	**31.14**	38.86	**44.37**	43.2	37.94
	PGD10-4	0.97	9.1	6.15	**9.91**	37.76	**43.43**	42.39	37.61
	PGD10-8	0	**3.32**	1.3	**3.35**	22.41	**29.09**	27.13	24.77
	PGD10-16	0	0.7	0	1	7.47	**13.18**	11.21	10.28
	PGD20-4	0	2.9	1.94	**3.15**	36.89	**42.65**	41.3	36.83
	PGD20-8	0	0.69	0.15	0.87	20.46	**26.89**	24.75	23.12
	PGD20-16	0	0	0	0	5.43	**9.82**	8.02	8.01
	PGD40-4	0	1.08	0.87	1.35	36.55	**42.45**	41.08	36.45
	PGD40-8	0	0.1	0	0	19.62	**26.1**	24.05	22.6
	PGD40-16	0	0	0	0	4.73	**8.22**	6.69	7.26
Black-Box	PGD10-4	13.77	18.07	21.36	18.44	49.4	52.25	**52.97**	46.76
	PGD10-8	3.65	5.45	**7.07**	5.6	38.84	**41.48**	41.44	38.55
	PGD20-4	9.92	13.31	**16.12**	13.5	49.34	52.02	**52.56**	46.45
	PGD20-8	1.89	2.84	**3.7**	2.98	38.25	**40.66**	40.39	38.13

Table 7: Performance under various attacks on CIFAR-100 (%). 0 denotes $< 0.1\%$

SVHN Mode	Attacks	Normal	Without AT			With AT			
			EntM	ADP	LS	PAT	PAT-EntM	PAT-LS	TRADES
White-Box	Clean	97.04	97.18	**97.58**	97.31	94	**94.08**	**94.08**	93.28
	FGSM4	65.74	85.39	83.55	**85.75**	82.99	83.21	83.04	**84.26**
	PGD10-4	27.54	*72.99*	*70.76*	***79.86***	79.72	80.11	79.39	**80.41**
	PGD10-8	4.73	48.47	*49.91*	***59.13***	61.71	63.88	62.6	**64.95**
	PGD10-16	0	21.61	25.13	**31.97**	29.33	**38.85**	35.77	36.27
	PGD20-4	13.04	55.47	54.68	**61.34**	78.15	**78.66**	77.55	78.45
	PGD20-8	0.81	22.42	25.24	**27.35**	55.24	57.37	55.56	**58.13**
	PGD20-16	0	5.0	6.6	7.2	18.65	**27.57**	23.9	24.49
	PGD40-4	8.37	40.85	42.73	**44.53**	77.71	**78.3**	77.06	77.96
	PGD40-8	0.36	10.27	**13.62**	12.4	52.76	54.65	52.14	**57.02**
	PGD40-16	0	1.15	2.25	1.9	14.18	**23.8**	17.58	17.96
Black-Box	PGD10-4	66.07	**70.47**	67.83	69.76	83.69	83.85	**84.08**	83.78
	PGD10-8	43.7	**49.77**	46.53	48.25	68.88	69.03	**69.48**	69.4
	PGD20-4	60.17	**66.33**	63.79	65.8	82.67	83.15	**83.3**	82.94
	PGD20-8	36.1	**45.3**	40.18	43.05	65.00	**65.42**	**65.43**	65.32

Table 8: Performance under various attacks on SVHN (%). 0 denotes $< 0.1\%$. Italics indicate white-box accuracies higher than corresponding black-box ones.

C.1 Random Searching

We present other evidence that EntM, LS and ADP alone may sometimes lead to gradient obfuscation. We sample 1000 images from the test set of CIFAR-10. We carry out random search attacks for 10,000 times on each image where EntM, LS and ADP succeeded in defending, and list the success rate of random attacks in Table 10. In many seemingly successful defenses (15% on LS, 6% on ADP and EntM), gradient-based attackers are obfuscated that they cannot find adversarial examples while such examples do exist. For reference, a PAT model shows no sign of gradient obfuscation.

We also perform exactly the same experiments for PAT and PAT-EntM. For samples where PAT and PAT-EntM succeeded in defending, *none* of them can be successfully attacked via a 10,000-time random search attack. It endorses that PAT-EntM is not suffering from gradient obfuscation.

MNIST Mode	Attacks	Normal	Without AT		With AT		
			EntM	ADP	PAT	PAT-EntM	TRADES
White-Box	Clean	99.2	99.13	**99.37**	**98.47**	98.04	97.78
	FGSM32	55.31	62.77	**77.61**	95.14	95.01	**95.18**
	PGD10-32	26.03	32.73	**57.54**	94.15	94.1	**94.28**
	PGD10-48	2.35	3.08	**17.06**	89.82	**90.65**	90.57
	PGD20-32	20.38	23.32	**43.76**	93.91	93.91	**94.2**
	PGD20-48	1.13	1.28	7.34	88.62	89.77	**90.53**
	PGD40-32	19.04	19.89	**39.14**	93.54	93.88	**94.17**
	PGD40-48	0.98	0.85	4.52	88.39	89.59	**90.52**
Black-Box	PGD10-32	83.11	85.76	**87.07**	96.32	96.16	96.93
	PGD10-48	46.94	52.2	**52.77**	94.6	94.48	**95.79**
	PGD20-32	81.43	83.95	**84.88**	96.31	95.96	**96.81**
	PGD20-48	44.68	46.23	**46.81**	94.36	94.23	**95.45**

Table 9: Performance under various attacks on MNIST (%).

Models	EntM	ADP	LS	PAT
# PGD8 fails	368	289	487	493
Among which # Random succeeds	20	12	70	0

Table 10: Attack success rate of random searching attacks on CIFAR-10.

C.2 Loss Surface Visualization

We choose data-label pairs (X, y) from the CIFAR-10 test set, and plot its local loss surface at $X' = X + \epsilon_1 d_1 + \epsilon_2 d_2$ to visually show the properties of EntM and PAT-EntM. $d_1 = \text{sign}\left(\nabla_X \text{CE}(f_\sigma(X;\theta), y)\right)$ is the gradient sign direction, and d_2 is a random direction with $\|d_2\|_\infty = 1$. We choose $\epsilon_1, \epsilon_2 \in [-0.04, 0.04]$.

Among the first 8 samples in the CIFAR-10 test set, we select 2 of them and plot them in Fig. 5. It can be shown that EntM alone is likely (25% would be a rough estimation.) to create a 'hole' in a small neighborhood of X, thereby causing gradient-based iterative attackers to stuck. This result corresponds with the fact that weak gradient-based attackers cannot achieve a high success rate due to gradient obfuscation. It also corresponds to the results in Table 4 that EntM alone may compromise local linearity by creating a highly curved surface.

We also plot the decision margin $M_{f,X'}$ at $X' = X + \epsilon_1 d_1 + \epsilon_2 d_2$ in Fig. 6. It can be shown that although EntM alone creates a small neighborhood where the margin is large, the area of the neighborhood is small, leaving large areas where $M_{f,X} = 0$. It shows that EntM alone cannot ensure robustness, especially when perturbations are large, and corresponds with results in Table 1, 2, 3.

D TRADES with EntM

We also carry out experiments on CIFAR-10 and CIFAR-100 to see how EntM works with TRADES. We take $\lambda = 2$ and list the results in Table 11 and 12. It can be shown that TRADES-EntM improves accuracy on clean examples by 6% on CIFAR-100 and 1.7% on CIFAR-10 compared to TRADES, but the robustness improvements are less evident than PAT-EntM, e.g. less than 1% improvement compared to TRADES under attacks on CIFAR-10, and 2-4% improvements on CIFAR-100.

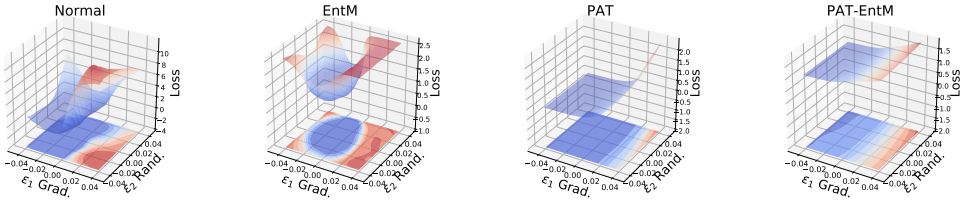

(a) Normal (b) EntM (c) PAT (d) PAT-EntM

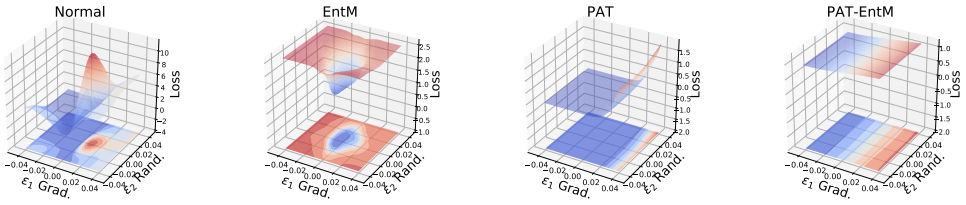

(e) Normal (f) EntM (g) PAT (h) PAT-EntM

Figure 5: Loss surface visualization at $X' = X + \epsilon_1 d_1 + \epsilon_2 d_2$ for for two X taken from the first 8 images in CIFAR-10 test set.

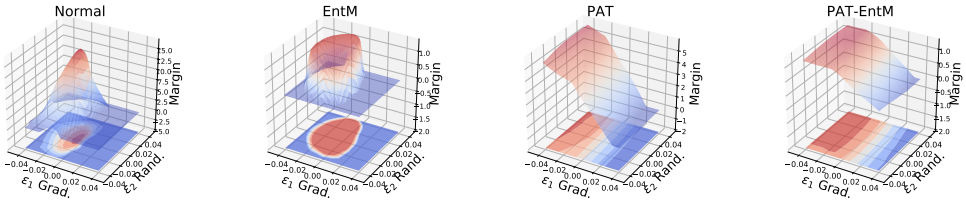

(a) Normal (b) EntM (c) PAT (d) PAT-EntM

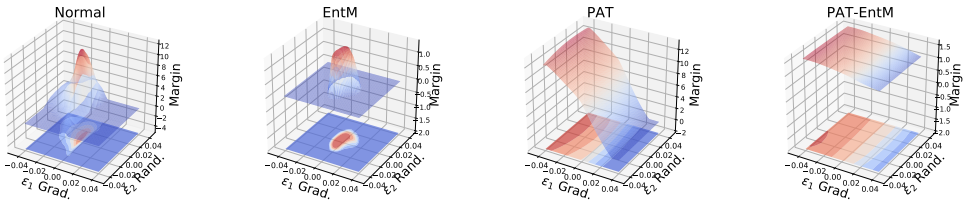

(e) Normal (f) EntM (g) PAT (h) PAT-EntM

Figure 6: Decision margin visualization at $X' = X + \epsilon_1 d_1 + \epsilon_2 d_2$ for two X taken from the first 8 images in CIFAR-10 test set.

CIFAR-10		PAT	TRADES	PAT-EntM	TRADES-EntM
White-Box	Clean	86.47	84.01	**87.87**	85.76
	FGSM4	70.33	69.21	**72.96**	70.43
	PGD10-4	68.33	68.72	**71.48**	69.48
	PGD10-8	48.87	51.35	**53.89**	51.56
	PGD10-16	19.63	25.77	**33.65**	26.47
	PGD20-4	67.89	67.58	**70.1**	68.83
	PGD20-8	44.61	47.82	**48.72**	48.18
	PGD20-16	12.76	18.27	**24.79**	19.01
	PGD40-4	67.51	67.4	**69.63**	68.64
	PGD40-8	43.03	**46.74**	45.95	46.43
	PGD40-16	10.26	15.27	**19.56**	15.14
Black-Box	PGD10-4	76.88	75.52	**79.32**	77.09
	PGD10-8	63.9	64.8	**65.82**	65.10
	PGD20-4	76.73	74.84	**78.67**	76.81
	PGD20-8	62.24	63.65	**64.44**	63.92

Table 11: TRADES-EntM in comparison with PAT, TRADES and PAT-EntM on CIFAR-10

CIFAR-100		PAT	TRADES	PAT-EntM	TRADES-EntM
White-Box	Clean	59.65	54.63	**62.53**	60.96
	FGSM4	38.86	37.94	**44.37**	42.84
	PGD10-4	37.76	37.61	**42.39**	41.96
	PGD10-8	22.41	24.77	**29.09**	27.78
	PGD10-16	7.47	10.28	**13.18**	12.33
	PGD20-4	36.89	36.83	**42.65**	41.4
	PGD20-8	20.46	23.12	**26.89**	25.99
	PGD20-16	5.43	7.26	**9.82**	9.16
	PGD40-4	36.55	36.45	**42.45**	41.22
	PGD40-8	19.62	22.6	**26.1**	25,34
	PGD40-16	4.73	7.26	**8.22**	7.9
Black-Box	PGD10-4	49.4	46.76	**52.25**	50.08
	PGD10-8	38.84	38.55	**41.48**	39.37
	PGD20-4	49.34	46.45	**52.02**	48.12
	PGD20-8	38.25	38.13	**40.66**	39.01

Table 12: TRADES-EntM in comparison with PAT, TRADES and PAT-EntM on CIFAR-100